

Probing the mixing between sterile and tau neutrinos in the SHiP experiment

Ki-Young Choi,^a Sung Hyun Kim,^b Yeong Gyun Kim,^c Kang Young Lee,^b Kyong Sei Lee,^d Byung Do Park,^b Jong Yoon Sohn,^b Seong Moon Yoo^a and Chun Sil Yoon^b

^a*Department of Physics and Institute of Basic Science, Sungkyunkwan University, Suwon 16419, Korea*

^b*Department of Physics Education & Research Institute of Natural Science, Gyeongsang National University, Jinju 52828, Korea*

^c*Department of Science Education, Gwangju National University of Education, Gwangju 61204, Korea*

^d*Center for Extreme Nuclear Matters, Korea University, Seoul 02841, Korea*

E-mail: kiyoungchoi@skku.edu, castledoor@skku.edu

ABSTRACT: We study the expected sensitivity to the mixing between sterile and tau neutrinos directly from the tau neutrino disappearance in the high-energy fixed target experiment. Here, the beam energy is large enough to produce tau neutrinos at the target with large luminosity. During their propagation to the detector, the tau neutrino may oscillate into sterile neutrino. By examining the energy spectrum of the observed tau neutrino events, we can probe the mixing between sterile and tau neutrinos directly. In this paper, we consider Scattering and Neutrino Detector (SND) at SHiP experiment as a showcase, which uses 400 GeV protons from SPS at CERN, and expect to observe 6,300 tau and anti-tau neutrinos from the 2×10^{20} POT for 5 years operation. Assuming the uncertainty of 10%, we find the sensitivity $|U_{\tau 4}|^2 \sim 0.08$ (90% CL) for $\Delta m_{41}^2 \sim 500 \text{ eV}^2$ with 10% signal-to-background ratio. We also consider a far SND at the end of the SHiP hidden sector detector, in which case the sensitivity would be enhanced to $|U_{\tau 4}|^2 \sim 0.02$.

Contents

1	Introduction	1
2	Neutrino Oscillation with Sterile Neutrino	2
3	Tau Neutrino Spectrum at the SHiP Experiment	3
4	Sensitivity to the Mixing between Sterile and Tau Neutrinos	5
5	Adding a Far Detector: NSND + FSND	9
6	Conclusion	11

1 Introduction

One of the simplest extensions to explain the neutrino mass is the introduction of additional right-handed neutrinos in the standard model [1–5]. These additional neutrinos should be free from the weak interaction [6], and thus they are called *sterile*. The sterile neutrinos may also explain the anomalies in the short baseline neutrino oscillation experiments [7, 8], and solve the cosmological problems of dark matter and baryon asymmetry [9].

The sterile neutrinos do not have weak interaction, however, they can communicate with visible sector through the mixing with active neutrinos at low energy. The resulting oscillation has been the main subject to search and constrain the sterile neutrinos [10, 11]. The mixing of sterile neutrino with electron and muon neutrino is constrained with a bound of $|U_{e4}|^2 \lesssim 0.04$ (90% CL) for $\Delta m_{41}^2 \sim 10^{-2} \text{ eV}^2$ and $|U_{\mu 4}|^2 \lesssim 10^{-2}$ for $10^{-2} \text{ eV}^2 \lesssim \Delta m_{41}^2 \lesssim 1 \text{ eV}^2$ [12].

About the mixing between sterile and tau neutrinos, two-neutrino oscillations of tau neutrinos are constrained by tau neutrino appearance. For instance, the constraint of $\nu_\mu \rightarrow \nu_\tau$ appearance from the NOMAD [13] and CHORUS experiments [14] give $4|U_{\mu 4}|^2|U_{\tau 4}|^2 < 5 \times 10^{-4}$ for $\Delta m_{41}^2 \gtrsim 100 \text{ eV}^2$ while the OPERA experiment [15], with its long baseline, probe it down to the mass $\Delta m_{41}^2 \gtrsim 0.02 \text{ eV}^2$ with a bound $4|U_{\mu 4}|^2|U_{\tau 4}|^2 < 0.116$. Constraints on $|U_{\tau 4}|^2$ only, in contrast, are much weaker than other active flavors since the best way to constrain the mixing to date is through the indirect disappearance of muon neutrinos under a long baseline [11, 16]. For instance, atmospheric neutrino experiments can provide constraints as $|U_{\tau 4}|^2 < 0.18$ in Super-Kamiokande [17] and $|U_{\tau 4}|^2 < 0.15$ in IceCube-DeepCore [18], for $\Delta m_{41}^2 \gtrsim 1 \text{ eV}^2$. Also, this mixing can be probed directly in neutral current interactions at the NOvA [19] and DUNE experiments [20], but sensitivities are weaker than the sensitivity from IceCube-DeepCore.

In this paper, to overcome such insensitive nature of $|U_{\tau 4}|^2$, we propose a new approach to constrain the mixing between sterile and tau neutrinos focusing on the SHiP experiment.

SHiP experiment is a facility that has been proposed at the SPS beam dump to search for hidden sectors beyond the SM [21–25]. Considering SND at SHiP as a short baseline, we can search for the evidence of tau neutrino disappearance during the propagation. Thanks to the high potential to detect $\mathcal{O}(10^4)$ tau neutrino Charged-Current(CC) events, it is possible to probe the mixing between sterile and tau neutrinos directly by measuring the tau neutrino energy spectrum.

The rest of this paper is organised as follows. In Sec. 2, we review the neutrino oscillation with sterile neutrino, and in Sec. 3 we summarise the SHiP experiment and show the expected energy spectrum of tau neutrino events. In Sec. 4, we describe the statistical method we employed and presents the expected sensitivity to the mixing between sterile neutrinos and tau neutrinos. In Sec. 5, we propose a new SND with long baseline that is placed after Hidden Sector Decay Spectrometer and estimate the enhancement of sensitivities due to the new SND. Lastly, we make a conclusion in Sec. 6.

2 Neutrino Oscillation with Sterile Neutrino

The weak eigenstates of neutrino $|\nu_\alpha\rangle$ is the linear combination of the mass eigenstates $|\nu_i\rangle$ determined by the mixing matrix \mathbf{U} ,

$$|\nu_\alpha\rangle = \sum_i U_{\alpha i}^* |\nu_i\rangle. \quad (2.1)$$

In ‘3+1’ model with single sterile neutrino as well as 3 active neutrinos in SM, the matrix becomes 4×4 matrix, which can be written as

$$\mathbf{U} = \begin{pmatrix} U_{e1} & U_{e2} & U_{e3} & U_{e4} \\ U_{\mu1} & U_{\mu2} & U_{\mu3} & U_{\mu4} \\ U_{\tau1} & U_{\tau2} & U_{\tau3} & U_{\tau4} \\ U_{s1} & U_{s2} & U_{s3} & U_{s4} \end{pmatrix}. \quad (2.2)$$

This mixing matrix can be parameterized with six rotation angles and three CP phases. The rotation angles include three additional mixing angles between the sterile neutrino and each active neutrino, θ_{14} , θ_{24} and θ_{34} as well as the usual three mixing angles between active neutrinos θ_{12} , θ_{23} and θ_{13} .

After travelling a distance L , the state of the neutrino evolves as

$$|\nu_\alpha(t)\rangle = \sum_i U_{\alpha i}^* |\nu_i(t)\rangle, \quad (2.3)$$

and the probability for the transition is given by

$$P_{\alpha\beta} = |\langle\nu_\beta|\nu_\alpha(t)\rangle|^2 = \left| \sum_{i,j} U_{\alpha i}^* U_{\beta j} \langle\nu_j|\nu_i(t)\rangle \right|^2. \quad (2.4)$$

Especially, for the short baseline experiment where the mixing between active neutrinos can be ignored, the probability of the relativistic neutrino can be approximated as

$$P_{\alpha\beta} = \left| \delta_{\alpha\beta} - \left(1 - e^{-i \frac{\Delta m_{41}^2 L}{2E_\nu}} \right) U_{\alpha 4} U_{\beta 4}^* \right|^2, \quad (2.5)$$

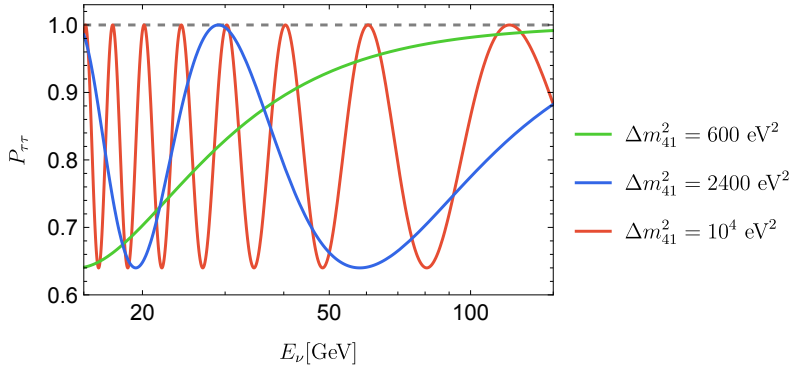


Figure 1. The survival probability of tau neutrinos, $P_{\tau\tau}$, for a mixing parameter of $|U_{\tau 4}|^2 = 0.1$ with a neutrino detector at a distance $L = 30$ m from the target. The different colors show the probability for different sterile neutrino masses: green, blue, and red line for $\Delta m_{41}^2 = 600, 2400, 10^4$ eV 2 , respectively. The dashed gray line represents $P_{\tau\tau} = 1$, for the case without mixing between tau neutrino and sterile neutrino.

where $\Delta m_{41}^2 \equiv m_4^2 - m_1^2$ is the mass squared difference between the sterile neutrino and the lightest neutrino, L is the baseline distance, and E_ν is the energy of the neutrino.

For tau neutrino disappearance experiments, the survival probability becomes

$$P_{\tau\tau} = 1 - 4|U_{\tau 4}|^2(1 - |U_{\tau 4}|^2) \sin^2 \left(\frac{\Delta m_{41}^2 L}{4E_\nu} \right), \quad (2.6)$$

where $|U_{\tau 4}|^2 = \sin^2 \theta_{34}^2$, ignoring other mixing angles.

In Fig. 1, we show the survival probability of tau neutrinos, $P_{\tau\tau}$, for a mixing parameter of $|U_{\tau 4}|^2 = 0.1$ with a neutrino detector at a distance $L = 30$ m from the target. The different colors show the probability for different sterile neutrino masses: green, blue, and red line for $\Delta m_{41}^2 = 600, 2400, \text{ and } 10^4$ eV 2 , respectively. The dashed gray line represents $P_{\tau\tau} = 1$, for the case without mixing between tau neutrinos and sterile neutrinos.

3 Tau Neutrino Spectrum at the SHiP Experiment

In the SHiP experiment, the high energy protons of 400 GeV from SPS can generate all three flavors of neutrino, when the protons are stopped at tungsten target. The neutrinos propagate through the shielding to the SND located 30 m away from the proton target. Three different flavors of neutrino can be observed using CC interaction at the emulsion detector in the SND.

While the electron and muon neutrinos are primarily produced from kaon and pion decays at the target, the tau neutrinos are mainly from the decay of the charm meson, $D_s \rightarrow \tau \nu_\tau$, and subsequent tau decays. The subsequent interaction of secondary particles, which we call cascade interaction, also can produce tau neutrinos¹. The number of tau

¹Including cascade interaction, the total number of charm meson is increased by a factor of 2.3 [26], but the detected number of ν_τ CC events would not increase much as the number of charm meson, since the angle and the energy of secondary tau neutrino is more dispersed than the primary tau neutrino. In this paper, we use the enhancement factor of 1.3, as suggested by Ref. [27].

neutrinos produced at the target can be estimated using Monte Carlo(MC) simulation of the experiment, and it could be around 10^{16} for 5 years operation [25].

The differential number of events of tau neutrinos with CC interaction at SND, with respect to the traveling distance and the energy of tau neutrino can be obtained by

$$\frac{d^2N}{dE_\nu dl} = n_W \frac{L_W}{L_{\text{SND}}} \epsilon_{\text{eff}} (\phi_{\nu_\tau} \sigma_{\nu_\tau A} + \phi_{\bar{\nu}_\tau} \sigma_{\bar{\nu}_\tau A}), \quad (3.1)$$

where n_W is the number density of tungsten atom in tungsten layers with total thickness L_W in SND, which length is L_{SND} . ϕ_{ν_τ} ($\phi_{\bar{\nu}_\tau}$) is the expected number of tau (anti) neutrinos passed through SND per E_ν , $\sigma_{\nu A}$ ($\sigma_{\bar{\nu} A}$) is the cross-section of (anti) neutrino-nucleus interaction, and ϵ_{eff} is the detection efficiency of tau neutrino. Here, the survival probability $P_{\tau\tau}(E_\nu, l)$ depends on the neutrino energy and the distance from the proton target.

Instead of full MC simulation, we adopt the event rate of tau neutrino CC interaction on 3 flavor model from Ref. [28], which is the most conservative result to the best of our knowledge. From here, we can write $\frac{dN}{dE_\nu}$ with sterile neutrino oscillation as

$$\frac{dN}{dE_\nu} = \int_{L_0}^{L_0+L_{\text{SND}}} P_{\tau\tau}(E_\nu, l) \frac{d^2N}{dE_\nu dl} dl, \quad (3.2)$$

where L_0 is the distance between the target and SND. Since the design of SND on Ref. [28] is similar with the design on the technical proposal of SHiP experiment at 2015 [21], we adopt ϵ_{eff} from the technical proposal at 2015, while $L_W = 100$ cm, $L_{\text{SND}} = 3$ m and $L_0 = 30$ m, following recent designs of SND at SHiP experiment [24, 25]. Therefore, after 5 years operation with 2×10^{20} POT, about 6,300 tau neutrino events are expected to be observed in the 3 flavor model.

To consider the energy response of SND in the reconstructed neutrino energy E_{rec} from the true energy E_ν , we used the reconstructed energy spectrum as

$$\frac{dN}{dE_{\text{rec}}} = \int_{E_\nu=0}^{\infty} f(E_{\text{rec}}, E_\nu) \frac{dN}{dE_\nu} dE_\nu, \quad (3.3)$$

where the Gaussian response function $f(E_{\text{rec}}, E_\nu)$ is given by

$$f(E_{\text{rec}}, E_\nu) \equiv \frac{1}{\sqrt{2\pi}\sigma} e^{-\frac{(E_\nu - E_{\text{rec}})^2}{2\sigma^2}}. \quad (3.4)$$

The energy classification from the hadron contribution determines σ , which we used as 20% of E_ν , *i.e.* $\sigma = 0.2E_\nu$, following the result from the technical proposal of SND@LHC. [29]

Note that, apart from the energy response, the baseline uncertainty also exists. This uncertainty comes from the varying interaction lengths between the target and the protons from SPS. However, this uncertainty is relatively minor compared to the length of SND, and can be ignored in our analysis.

In Fig. 2, we show the number of tau neutrino + tau anti neutrino events per energy at SND with respect to E_{rec} , considering the sterile neutrino oscillation for three mass squared differences, *i.e.* $\Delta m_{41}^2 = 600, 2400, \text{ and } 10^4 \text{ eV}^2$ with green, blue, and red colors, respectively. We can see the depletion of the probability depending on the energy of the neutrino, due to the oscillation into sterile neutrino.

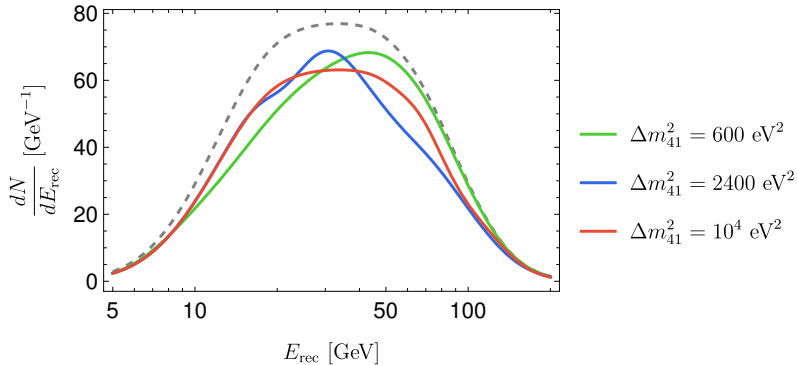


Figure 2. Differential number of distinguished ν_τ CC events on SND with respect to the reconstructed energy E_{rec} , if a mixing parameter $|U_{\tau 4}|^2 = 0.1$. Different scenarios are depicted: the green line for $\Delta m_{41}^2 = 600 \text{ eV}^2$, the blue line for $\Delta m_{41}^2 = 2400 \text{ eV}^2$, and the dashed red line for $\Delta m_{41}^2 = 10^4 \text{ eV}^2$. The dashed gray line represents the case with $P_{\tau\tau} = 1$, indicating no mixing between tau neutrino and sterile neutrino.

4 Sensitivity to the Mixing between Sterile and Tau Neutrinos

In this section, we show the expected sensitivity to ‘3+1’ model using the tau neutrino disappearance at SHiP experiment. To find the expected sensitivity, we assumed that the result from SHiP experiment is in agreement with the standard three neutrino model and found the Confidence Level (CL) of the virtual result at each point of ‘3+1’ model parameters. To find the CL, we used two different methods: 1) Wilks’ theorem [30], and 2) the profiled Feldman-Cousins (FC) method [31, 32].

We use the well-known statistic $\Delta\chi^2$ which quantifies the fitness of the data with the corresponding model, defined as

$$\Delta\chi^2 \equiv \chi_{\lambda}^2 - \chi_{\theta, \lambda}^2, \quad (4.1)$$

where $\chi_{\mathbf{a}}^2 \equiv -2 \max_{\mathbf{a}} \log L$, which maximises the likelihood function L for any set of parameters \mathbf{a} . For a likelihood function from SHiP experiment, we use Poisson probability distributions $\text{Pois}(O_i|\mu_i)$, and a likelihood function for the nuisance parameters from previous experiments $L(\boldsymbol{\lambda})$, which confines their possible range with uncertainties of SHiP experiment. The combined likelihood function of a data \mathbf{O} for model parameters $\boldsymbol{\theta}$ and nuisance parameters $\boldsymbol{\lambda}$ is written as

$$L(\boldsymbol{\theta}, \boldsymbol{\lambda}|\mathbf{O}) = L(\boldsymbol{\lambda}) \times \prod_{i \in \text{bin}} \text{Pois}(O_i|\mu_i), \quad (4.2)$$

where O_i and μ_i are the observed and expected number of ν_τ CC events at a i -th bin. The number of events at i -th bin $\mu_i \equiv s_i + b_i$ is the sum of signal s_i and background b_i , which is evaluated for given set of parameters $\boldsymbol{\theta}$ and $\boldsymbol{\lambda}$.

The expected number of signal at i -th bin is calculated as

$$s_i(\boldsymbol{\theta}) = (1 + A)(1 + \alpha_i) \int_{E_{i,\text{low}}}^{E_{i,\text{high}}} \frac{dN}{dE_{\text{rec}}} \Big|_{\boldsymbol{\theta}} dE_{\text{rec}}, \quad (4.3)$$

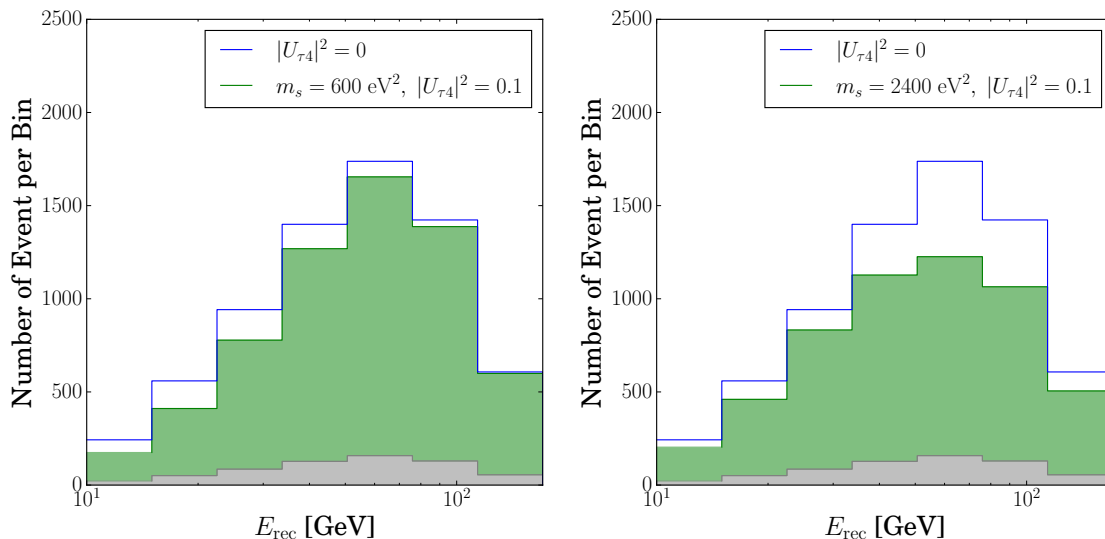


Figure 3. Number of expected event per bin with the mixing $|U_{\tau 4}|^2 = 0.1$, assuming 10% background (grey color with $R_{s/b} = 10$) for $\Delta m_{41}^2 = 600$ (left), and 2400 eV^2 (right). For a comparison, blue plot shows the most-probable pseudo data for 3 flavor model without sterile neutrino mixing.

where the nuisance parameters $A, \alpha_i \in \boldsymbol{\lambda}$ represent overall and shape uncertainties for signal, which are assumed to have a mean value of zero, while $E_{i,\text{low}}$ and $E_{i,\text{high}}$ are the lower and upper energy limit of i -th energy bin. Overall and shape uncertainties reflect the uncertainties from parton distributions, factorization and renormalization scale factor, intrinsic transverse momentum [22, 28, 33], and other possible experimental uncertainties. In this paper, we assume the likelihood function of nuisance parameters as similar as a normal distribution. For simplicity, all nuisance parameters are independent of each other and share the same variance σ_{norm}^2 during the analysis, even though the likelihood function may include non-zero covariance terms between nuisance parameters. Therefore, we rewrite $L(\boldsymbol{\lambda})$ as

$$L(\boldsymbol{\lambda}) \sim \prod_{\lambda \in \boldsymbol{\lambda}} \text{Exp} \left[-\frac{\lambda^2}{2\sigma_{\text{norm}}^2} \right]. \quad (4.4)$$

For the variance of nuisance parameters, we choose $\sigma_{\text{norm}} = 10\%$ or $\sigma_{\text{norm}} = 20\%$ in later figures. These uncertainties can be refined with the results from the DsTau Project in the future [34].

To consider the background, we use the tau neutrino spectrum divided by signal-to-background ratio $R_{s/b}$ in 3 flavor model ². Similar with A and α_i , we included a overall uncertainty $B \in \boldsymbol{\lambda}$ and shape uncertainties $\beta_i \in \boldsymbol{\lambda}$ in the background. Therefore, the

²For an appropriate treatment of the background, full MC simulation of the experiment and statistical analysis of MC data are needed, which is beyond our scope.

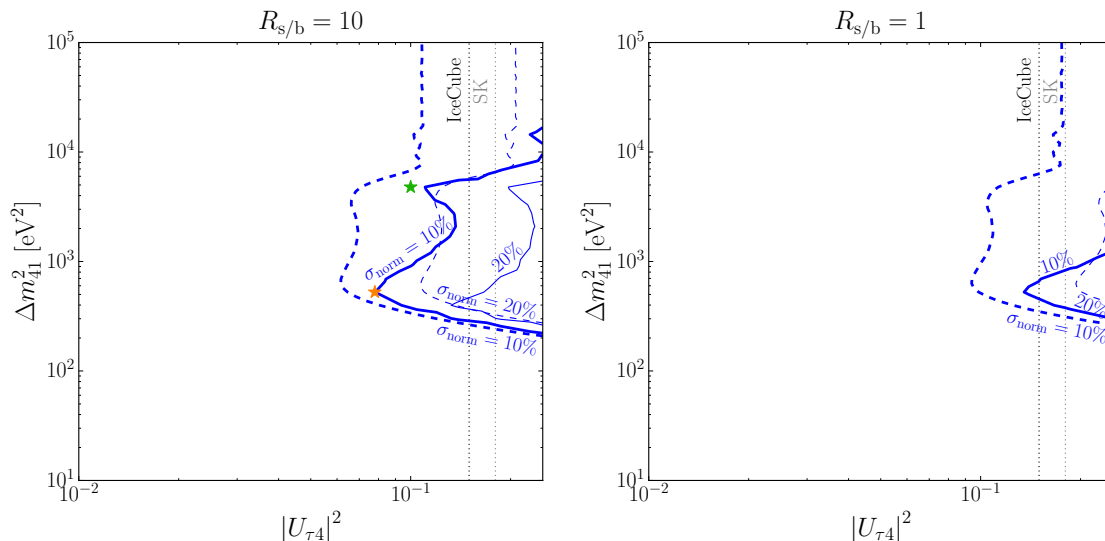


Figure 4. The expected sensitivity after 5 year observation at SHiP on the plane of $(|U_{\tau 4}|^2, \Delta m_{41}^2)$ under the assumption of $\theta_{14} = \theta_{24} = 0$, for different number of background $R_{s/b} = 10$ (left) and 1 (right). Blue solid (dashed) lines are the constraint of 90% CL using the profiled FC method (Wilks' theorem), with uncertainty $\sigma_{\text{norm}} = 10\%$ (thick lines) or 20% (thin lines). The vertical dashed lines show the existing constraints from IceCube-DeepCore [18] (black) and Super-Kamiokande [17] (grey), respectively. To check the validity of Wilks' theorem, CDFs of $\Delta\chi^2$ at orange and green stars on the left figure are drawn in Fig. 5.

expected number of the background at i -bin is written as

$$b_i = R_{s/b}^{-1}(1 + B)(1 + \beta_i) \int_{E_i^{\text{low}}}^{E_i^{\text{high}}} \frac{dN}{dE_{\text{rec}}} \Big|_{|U_{\tau 4}|^2=0} dE_{\text{rec}}. \quad (4.5)$$

Here, the background is independent of sterile neutrino parameters, and $R_{s/b}$ is chosen as 10 or 1 in later figures.

A logarithmic scale is used for our bins, beginning at 10 GeV and each bin ends at 1.5 times its starting energy, with a total of 7 bins. In Fig. 3, we show the number of expected events per bin (green) after 5 years operation with the mixing $|U_{\tau 4}|^2 = 0.1$, assuming 10% background ($R_{s/b} = 10$ with grey color) for $\Delta m_{41}^2 = 600 \text{ eV}^2$ (left) and 2400 eV^2 (right). For a comparison, the blue plot shows the most probable pseudo-data for the 3-neutrino model.

To find a CL, as a first method, we use Wilks' theorem [30], which points out that under certain conditions, the probability distribution of $\Delta\chi^2$ follows a χ^2 distribution with the same number of degrees of freedom as θ , which is 2 in this study since $\theta = (\Delta m_{41}^2, |U_{\tau 4}|^2)$. However, in neutrino oscillation models, the probability distribution of $\Delta\chi^2$ does not necessarily follows a χ^2 distribution. Therefore, as a second method, we utilized the profiled FC method [32] which is a variant of FC method [31] for a case with nuisance parameters. After choosing \mathbf{O} as most-probable data in 3 flavor model, we

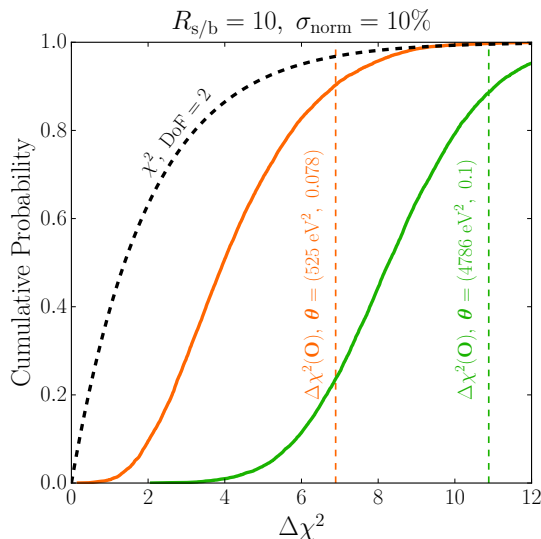


Figure 5. Cumulative distribution functions of χ^2 distribution with two degrees of freedom (dashed black) and distributions of $\Delta\chi^2$ using the profiled FC method, corresponding to star shaped points in Fig. 4 with $(\Delta m_{41}^2, |U_{\tau 4}|^2) = (525 \text{ eV}^2, 0.078)$ (orange), and $(4786 \text{ eV}^2, 0.1)$ (green), for $R_{s/b} = 10$ and $\sigma_{\text{norm}} = 10\%$. Vertical dashed lines indicate the value of $\Delta\chi^2(\mathbf{O})$ for each point.

generated 10^4 number of pseudo-data by MC simulation on each point θ on the map of model parameters, assuming $\lambda = \text{argmax}_{\lambda} L(\theta, \lambda | \mathbf{O})$. By calculating $\Delta\chi^2$ of each set of pseudo-data, we find its probability distribution which is denoted as $f(x)$.

From the probability distribution of $\Delta\chi^2$, the CL of the data \mathbf{O} is defined as follows:

$$\text{CL} = \int_0^{\Delta\chi^2(\mathbf{O})} f(x) dx, \quad (4.6)$$

where $\Delta\chi^2(\mathbf{O})$ is $\Delta\chi^2$ value of the data \mathbf{O} . Here, the definition of a CL indicates the possibility that other possible outcome from the same experiment would give a better fit, more than the data \mathbf{O} . The range of integration in Eq. (4.6) starts at $x = 0$, as $\Delta\chi^2$ must be non-negative according to the definition.

In Fig. 4, we show the expected sensitivity after 5 year observation at SHiP on the plane of $(|U_{\tau 4}|^2, \Delta m_{41}^2)$ under the assumption of $\theta_{14} = \theta_{24} = 0$, for different number of background $R_{s/b} = 10$ (left) and 1 (right). Uncertainties of nuisance parameters are chosen as $\sigma_{\text{norm}} = 10\%$ (thick lines) and 20% (thin lines), while solid (dashed) lines are the constraint of 90% CL using the profiled FC method (Wilks' theorem). Wilks' theorem is applied by drawing a contour of $\Delta\chi^2 = 4.61$, which corresponds to first 90% cut of χ^2 distribution with two degrees of freedom, while profiled FC method is applied through drawing a contour of 90% CL using Eq. (4.6). The vertical dashed lines show the existing constraints from IceCube-DeepCore [18] and Super-Kamiokande [17], respectively.

From the left window in Fig. 4, we can find the sensitivity using profiled FC method could be $|U_{\tau 4}|^2 \sim 0.08$ (0.1) for $\Delta m_{41}^2 \sim 500 \text{ eV}^2$ with uncertainty 10% (20%), respectively, after 5 year operation of SHiP experiment with 10% background. For $\Delta m_{41}^2 \gtrsim 500 \text{ eV}^2$,

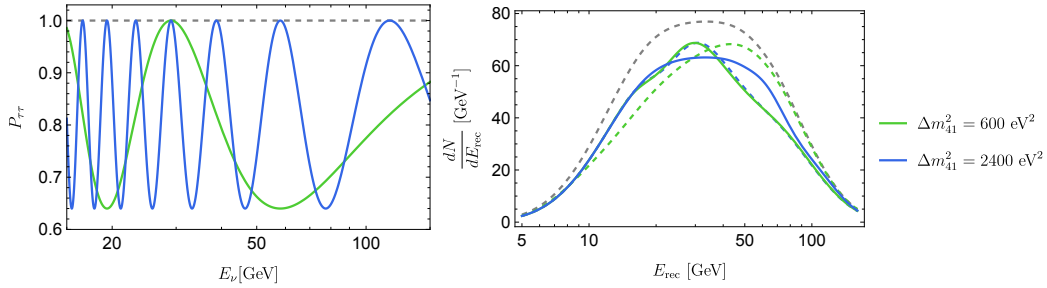


Figure 6. (Left) Survival probability of tau neutrinos as a function of E_ν at 120 m baseline. (Right) Differential number of ν_τ CC events at FSND, assuming the same number of event as expected in NSND, *i.e.* $R_{F/N} = 100\%$. In both figures, the green line stands for $\Delta m_{41}^2 = 600 \text{ eV}^2$ and blue line for $\Delta m_{41}^2 = 2400 \text{ eV}^2$. In the right figure, the dashed lines are the spectrum at NSND for the corresponding mass difference, with black dashed line for the spectrum without oscillation with sterile neutrino.

in general, there is inconsistency between the sensitivities from Wilks' theorem and the profiled FC method, indicating that the probability distribution function $f(x)$ on Eq. (4.6) from the profiled FC method does not follow χ^2 distribution.

In Fig. 5, we show Cumulative Distribution Function (CDF)s of $\Delta\chi^2$ using profiled FC method corresponding to two star-shaped points in Fig. 4 (solid orange and green), with that of χ^2 distribution with two degrees of freedom (dashed black). The value of $\Delta\chi^2(\mathcal{O})$ is displayed with vertical dashed lines with the corresponding colors. We can check that for these points the Wilks' theorem is not applied well and thus the sensitivities between profile FC and Wilks' theorem show discrepancy.

5 Adding a Far Detector: NSND + FSND

In this section, we consider an additional SND with longer baseline, which we call far SND (FSND), to enhance the sensitivity. The distance from the proton target to FSND we assumed is 120 m, therefore FSND will be placed after Hidden Sector Decay Spectrometer in the current design of SHiP experiment. For comparison, we refer to the SND positioned closer to the proton target as near SND (NSND). Since the disappearance pattern of tau neutrinos from '3+1' model is dependent on the baseline while nuisance parameters are not, introducing FSND gives more control on nuisance parameters.

For simplicity, we assume that the projected geometry of FSND is the same as NSND, but the vertical length of FSND can be adjusted. Depending on the vertical length of FSND, we consider several different acceptance of FSND, quantified by a parameter $R_{F/N}$ which denotes the ratio of ν_τ CC events at FSND compared to NSND. In Fig. 6, we show the survival probability of tau neutrinos at the 120 m baseline (left) and differential number of ν_τ CC events at FSND (right) with $\Delta m_{41}^2 = 600 \text{ eV}^2$ (green) and $\Delta m_{41}^2 = 2400 \text{ eV}^2$ (blue) if FSND has the same expected number of events as NSND, *i.e.* $R_{F/N} = 100\%$. For comparison, the differential number of ν_τ CC events at NSND from Fig. 2 are shown

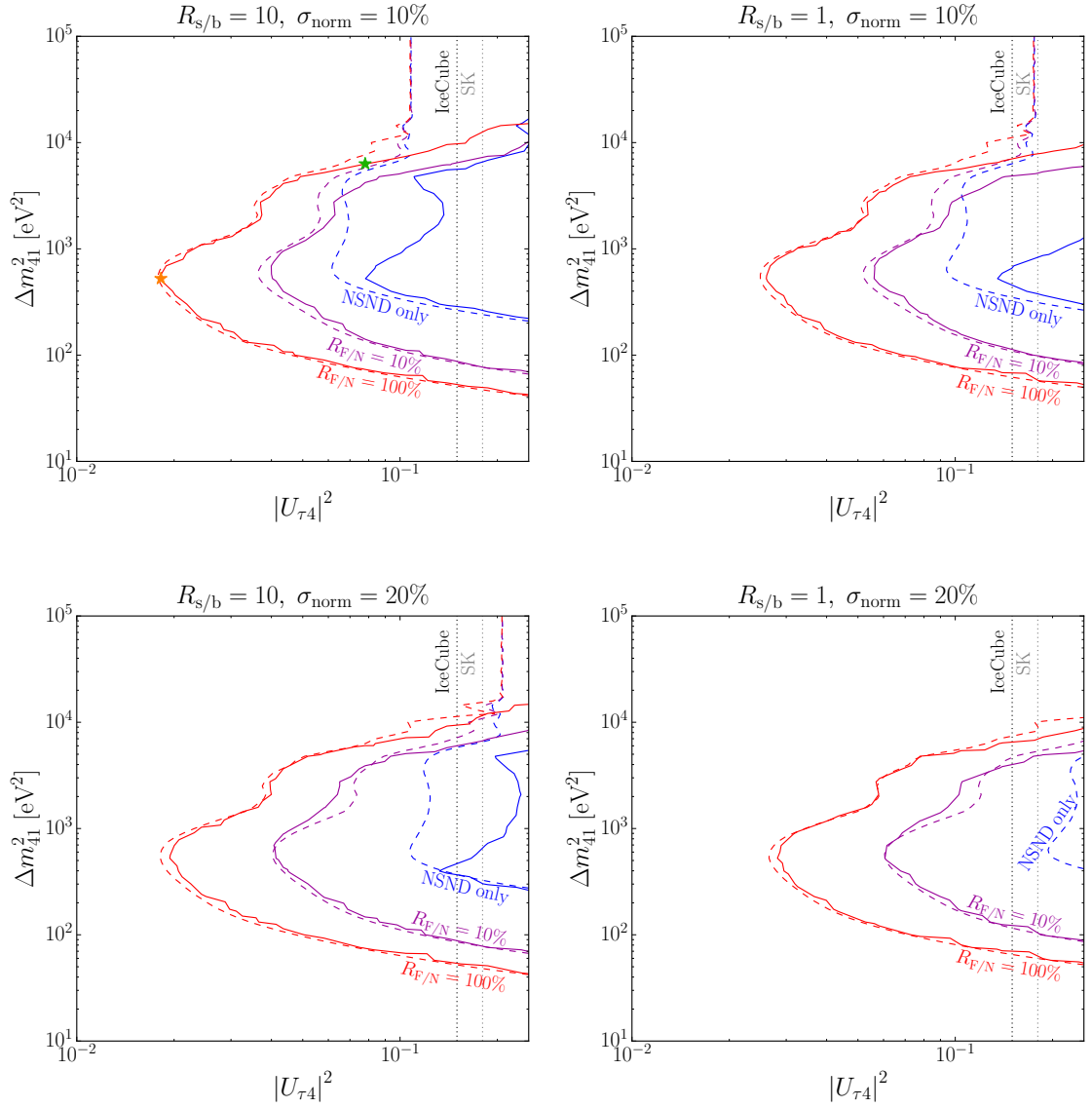


Figure 7. The same as Fig. 4 but with the combined analysis with both NSND and FSND for different $R_{F/N}$ values, 10% (purple) and 100% (red) as well as NSND only (blue). In the upper (lower) windows $\sigma_{\text{norm}} = 10\%$ (20%), and in the left (right) windows $R_{s/b} = 10$ (1) is used. Like Fig. 4, solid (dashed) lines indicates that the profiled FC method (Wilks' theorem) is used to find the CL.

with dashed lines with corresponding colors. We can see the clear change of spectrum from NSND to FSND.

In Fig. 7, we show the expected sensitivity to $|U_{\tau 4}|^2$ and Δm_{41}^2 with the combined data from NSND and FSND for different geometric acceptance at FSND, $R_{F/N} = 10\%$, 100%, and also include results from NSND only case for comparison. In the upper (lower) windows $\sigma_{\text{norm}} = 10\%$ (20%) is used, and in the left (right) windows $R_{s/b} = 10$ (1) is used. Compared

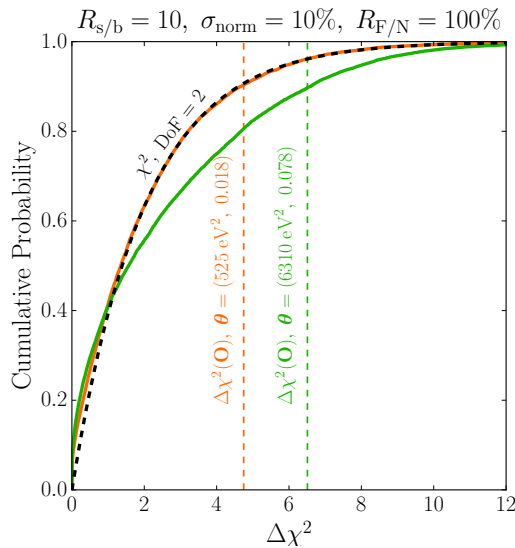


Figure 8. CDFs of χ^2 distribution with two degrees of freedom (dashed black) and distributions of $\Delta\chi^2$ using the profiled FC method, corresponding to star shaped points in Fig. 7 with $(\Delta m_{41}^2, |U_{\tau 4}|^2) = (525 \text{ eV}^2, 0.018)$ (orange), and $(6310 \text{ eV}^2, 0.078)$ (green), for $R_{s/b} = 10$, $\sigma_{\text{norm}} = 10\%$ and $R_{F/N} = 100\%$. Vertical dashed lines indicate the value of $\Delta\chi^2(\mathbf{O})$ for each point.

to the NSND only case, both methods gives similar sensitivity near $\Delta m_{41}^2 \sim 10^3 \text{ eV}^2$, and it merely depends on σ_{norm} , meaning that the uncertainty from nuisance parameters can be relaxed. If $R_{F/N} = 100\%$ and $R_{s/b} = 10$ (1), the combined sensitivity from NSND+FSND can be $|U_{\tau 4}|^2 \sim 0.02$ (0.03) near $\Delta m_{41}^2 \sim 500 \text{ eV}^2$.

In Fig. 8, we show the CDFs of $\Delta\chi^2$ at orange and green stars on the upper-left window in Fig. 7. As can be seen from this figure, the CDFs from both method are consistent very well for the orange point, which explains the similar sensitivity with both methods in Fig. 7 for $\Delta m_{41}^2 \lesssim 5000 \text{ eV}^2$. For larger Δm_{41}^2 , sensitivities from both methods start to mismatch, as can be seen with the CDFs for the point of the green star.

6 Conclusion

In this paper, we considered tau neutrino disappearance for the first time in the high energy fixed target experiment of SHiP, where several thousand tau neutrinos are expected to be observed after 5 years operation. This gives good environment for the tau neutrino oscillation experiment.

We studied sterile neutrino oscillation in ‘3+1’ model and derived possible sensitivity to the mixing and mass difference using the energy spectrum of the tau (anti)neutrinos. With NSND only, the sensitivity would be $|U_{\tau 4}|^2 \sim 0.08$ (0.1) near $\Delta m_{41}^2 \sim 500 \text{ eV}^2$, for $\sigma_{\text{norm}} = 10\%$ (20%) and $R_{s/b} = 10$ using profiled FC method. We find that this is slightly weaker than the sensitivity assuming the Wilks’ theorem is applied.

To enhance the sensitivity, we suggested additional FSND which can be put after Hidden Sector Decay Spectrometer. It can play a role of far detector and its spectrum can be directly compared to that of NSND. From Fig. 7, NSND+FSND gives a robust sensitivity that does not depend on the choice of statistical method. Also, the constraints barely change with the choice of σ_{norm} . If $R_{\text{F/N}} = 100\%$, the combined data gives the sensitivity $|U_{\tau 4}|^2 \sim 0.02$ (0.03) near $\Delta m_{41}^2 \sim 500 \text{ eV}^2$ with $R_{s/b} = 10$ (1).

Acknowledgments

The authors deeply appreciate Yu Seon Jeong for useful discussion. The authors were supported by the National Research Foundation of Korea (NRF) grant funded by the Korea government (MEST) 2021R1A2C2011003, 2021R1F1A1061717, and 2022R1A2C100505.

References

- [1] P. Minkowski, $\mu \rightarrow e\gamma$ at a Rate of One Out of 10^9 Muon Decays?, *Phys. Lett. B* **67** (1977) 421.
- [2] P. Ramond, *The Family Group in Grand Unified Theories*, in *International Symposium on Fundamentals of Quantum Theory and Quantum Field Theory*, 2, 1979 [[hep-ph/9809459](#)].
- [3] M. Gell-Mann, P. Ramond and R. Slansky, *Complex Spinors and Unified Theories*, *Conf. Proc. C* **790927** (1979) 315 [[1306.4669](#)].
- [4] T. Yanagida, *Horizontal gauge symmetry and masses of neutrinos*, *Conf. Proc. C* **7902131** (1979) 95.
- [5] R.N. Mohapatra and G. Senjanovic, *Neutrino Mass and Spontaneous Parity Nonconservation*, *Phys. Rev. Lett.* **44** (1980) 912.
- [6] P. Janot and S. Jadach, *Improved Bhabha cross section at LEP and the number of light neutrino species*, *Phys. Lett. B* **803** (2020) 135319 [[1912.02067](#)].
- [7] LSND collaboration, *Evidence for neutrino oscillations from the observation of $\bar{\nu}_e$ appearance in a $\bar{\nu}_\mu$ beam*, *Phys. Rev. D* **64** (2001) 112007 [[hep-ex/0104049](#)].
- [8] MINIBOONE collaboration, *Updated MiniBooNE neutrino oscillation results with increased data and new background studies*, *Phys. Rev. D* **103** (2021) 052002 [[2006.16883](#)].
- [9] B. Dasgupta and J. Kopp, *Sterile Neutrinos*, *Phys. Rept.* **928** (2021) 1 [[2106.05913](#)].
- [10] M. Dentler et al., *Updated Global Analysis of Neutrino Oscillations in the Presence of eV-Scale Sterile Neutrinos*, *JHEP* **08** (2018) 010 [[1803.10661](#)].
- [11] M.A. Acero et al., *White Paper on Light Sterile Neutrino Searches and Related Phenomenology*, [2203.07323](#).
- [12] MINOS+, DAYA BAY collaboration, *Improved Constraints on Sterile Neutrino Mixing from Disappearance Searches in the MINOS, MINOS+, Daya Bay, and Bugey-3 Experiments*, *Phys. Rev. Lett.* **125** (2020) 071801 [[2002.00301](#)].
- [13] NOMAD collaboration, *Final NOMAD results on muon-neutrino \rightarrow tau-neutrino and electron-neutrino \rightarrow tau-neutrino oscillations including a new search for tau-neutrino appearance using hadronic tau decays*, *Nucl. Phys. B* **611** (2001) 3 [[hep-ex/0106102](#)].

- [14] CHORUS collaboration, *Final results on $\nu(\mu) \rightarrow \nu(\tau)$ oscillation from the CHORUS experiment*, *Nucl. Phys. B* **793** (2008) 326 [[0710.3361](#)].
- [15] OPERA collaboration, *Limits on muon-neutrino to tau-neutrino oscillations induced by a sterile neutrino state obtained by OPERA at the CNGS beam*, *JHEP* **06** (2015) 069 [[1503.01876](#)].
- [16] R. Mammen Abraham et al., *Tau neutrinos in the next decade: from GeV to EeV*, *J. Phys. G* **49** (2022) 110501 [[2203.05591](#)].
- [17] SUPER-KAMIOKANDE collaboration, *Limits on sterile neutrino mixing using atmospheric neutrinos in Super-Kamiokande*, *Phys. Rev. D* **91** (2015) 052019 [[1410.2008](#)].
- [18] ICECUBE collaboration, *Search for sterile neutrino mixing using three years of IceCube DeepCore data*, *Phys. Rev. D* **95** (2017) 112002 [[1702.05160](#)].
- [19] NOVA collaboration, *Search for Active-Sterile Antineutrino Mixing Using Neutral-Current Interactions with the NOvA Experiment*, *Phys. Rev. Lett.* **127** (2021) 201801 [[2106.04673](#)].
- [20] P. Coloma, D.V. Forero and S.J. Parke, *DUNE Sensitivities to the Mixing between Sterile and Tau Neutrinos*, *JHEP* **07** (2018) 079 [[1707.05348](#)].
- [21] SHiP collaboration, *A facility to Search for Hidden Particles (SHiP) at the CERN SPS*, [1504.04956](#).
- [22] S. Alekhin et al., *A facility to Search for Hidden Particles at the CERN SPS: the SHiP physics case*, *Rept. Prog. Phys.* **79** (2016) 124201 [[1504.04855](#)].
- [23] SHiP collaboration, *BDF/SHiP at the ECN3 high-intensity beam facility*, .
- [24] SHiP collaboration, *SHiP Experiment - Progress Report*, Tech. Rep. [CERN-SPSC-2019-010, SPSC-SR-248](#), CERN, Geneva (2019).
- [25] SHiP collaboration, *BDF/SHiP at the ECN3 high-intensity beam facility*, Tech. Rep. [CERN-SPSC-2023-033, SPSC-P-369](#), CERN, Geneva (2023).
- [26] SHiP collaboration, *Heavy Flavour Cascade Production in a Beam Dump*, .
- [27] A. Iuliano, *Event reconstruction and data analysis techniques for the SHiP experiment*, Ph.D. thesis, Università degli Studi di Napoli Federico II, 2021.
- [28] W. Bai and M.H. Reno, *Prompt neutrinos and intrinsic charm at SHiP*, *JHEP* **02** (2019) 077 [[1807.02746](#)].
- [29] C.e.a. Ahdida, *SND@LHC - Scattering and Neutrino Detector at the LHC*, Tech. Rep. [CERN-LHCC-2021-003, LHCC-P-016](#), CERN, Geneva (2021).
- [30] S.S. Wilks, *The Large-Sample Distribution of the Likelihood Ratio for Testing Composite Hypotheses*, *The Annals of Mathematical Statistics* **9** (1938) 60 .
- [31] G.J. Feldman and R.D. Cousins, *A Unified approach to the classical statistical analysis of small signals*, *Phys. Rev. D* **57** (1998) 3873 [[physics/9711021](#)].
- [32] NOvA collaboration, *The Profiled Feldman-Cousins technique for confidence interval construction in the presence of nuisance parameters*, [2207.14353](#).
- [33] R.E. Nelson, R. Vogt and A.D. Frawley, *Narrowing the uncertainty on the total charm cross section and its effect on the J/ψ cross section*, *Phys. Rev. C* **87** (2013) 014908 [[1210.4610](#)].
- [34] DS-TAU collaboration, *DsTau: Study of tau neutrino production with 400 GeV protons from the CERN-SPS*, *JHEP* **01** (2020) 033 [[1906.03487](#)].